



Synthesis, structural analysis and electrochemical performances of BLSITCF_x as new cathode materials for solid oxide fuel cells (SOFC) based on BIT07 electrolyte

M. Letilly^a, A. Le Gal La Salle^{a,*}, A. Lachgar^b, O. Joubert^a

^a Institut des Matériaux Jean Rouxel (IMN), CNRS– Université de Nantes, 2 rue de la Houssinière, BP 32229, 44322 Nantes, France

^b Department of Chemistry, Wake Forest University, Winston-Salem, NC 27109, USA

ARTICLE INFO

Article history:

Received 23 July 2009

Received in revised form 15 February 2010

Accepted 21 February 2010

Available online 26 February 2010

Keywords:

SOFC

Oxides

Complex impedance spectroscopy

Cathode

BIT07

ABSTRACT

Ba_{0.3}Ti_{0.7}O_{2.85} (BIT07) is a suitable electrolyte for Solid Oxide Fuel Cell (SOFC) but half cells based on La_{0.58}Sr_{0.4}Co_{0.2}Fe_{0.8}O_{3-δ} (LSCF) as a cathode material show a degradation of the Area Specific Resistance (ASR) at 700 °C with time. This study deals with the characterization of alternative cathode materials showing a better compatibility with BIT07 than LSCF. A new solid solution, Ba_xLa_{0.58(1-x)}Sr_{0.4(1-x)}In_{0.3x}Ti_{0.7x}Co_{0.2(1-x)}Fe_{0.8(1-x)}O_{3-δ}, with 0 ≤ x ≤ 1, also called BLSITCF_x, with in this case x expressed in molar %, derived from BIT07 and LSCF, has been synthesized at 1350 °C in air using BIT07 and LSCF powders. Two compositions, BLSITCF12 and BLSITCF25, have been selected due to their thermal expansion and conductivity properties. Symmetrical half cells based on these two new materials deposited on BIT07 electrolyte have been studied by complex impedance spectroscopy in air versus temperature and time. Their behaviour is comparable to LSCF's, with ASR values never exceeding 0.2 Ωcm² at 700 °C, and moreover their less important Thermal Expansion Coefficient (TEC) mismatch with BIT07 lead to a better mechanical compatibility with time. These new compounds are therefore better candidates than LSCF as cathode materials for SOFC based on BIT07 electrolyte.

© 2010 Elsevier B.V. All rights reserved.

1. Introduction

Solid oxide fuel cells (SOFC) are all-solid devices converting the chemical energy of gaseous fuels into electricity via electrochemical processes with high energy conversion efficiency and low greenhouse gas emission [1]. To develop the SOFC technology, its operating temperature has to be lowered, since at high temperatures (800–1000 °C), the fuel cell materials degradation is accelerated [2]. However, intermediate temperature SOFCs (ITSOFC) working at ≈700 °C exhibit quite low performances in terms of energy density, ionic conductivity of the electrolyte and ohmic drop at the cathode–electrolyte interface. To develop the ITSOFC technology, it is essential to reduce both the polarization and resistance losses of the cell. These contributions can be reduced significantly by using materials in the form of thin films, resulting in a decrease of the overall cell resistance [3,4]. Low polarization losses can also be achieved by employing electrode materials with high activity for the electrochemical reactions and by optimizing the microstructure in the electrode/electrolyte interface region.

Ba_{0.3}Ti_{0.7}O_{2.85} (BIT07) is an alternative electrolyte material for ITSOFC [5], because, below 700 °C, its ion conductivity level is comparable to that of YSZ, the usual electrolyte material. More-

over BIT07, which is a cubic perovskite type oxide, is expected to present an excellent structural compatibility with perovskite cathode substrates (e.g. LSM, LSCF...). In order to validate its use in SOFC, this material has to fulfill several criteria. First BIT07 has to be chemically compatible with usual cathode materials, second the assembly BIT07/cathode has to exhibit similar electrochemical performances to the actual very performing YSZ/cathode and thirdly it has to show long-term cycle life. In a previous study [6], it has been shown that BIT07 is compatible with the well-known cathode materials LSCF (La_{0.58}Sr_{0.4}Co_{0.2}Fe_{0.8}O_{3-δ}) [7–12] and can be used with this material without requiring the use of intermediate layers [13,14], which is time and cost-effective, as the design and the firing step of the intermediate layer is avoided. However, an ageing problem has been noticed, probably associated to the TEC mismatch between BIT07 and LSCF. In the same study, it has been shown that, at 1000 °C, a reaction between BIT07 and LSCF occurred, leading to the formation of a new single-phase compound with a perovskite type structure. This phase which appears at the electrolyte/cathode interface could show interesting characteristics such as ionic or electronic conductivity leading to an improvement of its mechanical properties without lowering the electrochemical performances of the assembly. In contrary, this phase could be an insulating layer at the cathode/electrolyte interface [15].

In order to go further, new compositions have been synthesized at high temperatures starting from different mixtures of BIT07 and

* Corresponding author. Tel.: +33 240373913; fax: +33 240373995.

E-mail address: annie.legal@cnrs-imn.fr (A. Le Gal La Salle).

LSCF. In this paper we present these new compounds which have been characterized and tested from electrochemical and mechanical points of view. Anode materials compatible with BIT07 have been prepared by the authors [16] and their optimization with these new materials will be published elsewhere.

2. Experimental

2.1. Sample preparation

BIT07 is synthesized as detailed in [5]: its constituents, high purity barium carbonate (Alfa Aesar, Germany), indium oxide (Alfa Aesar, Germany) and titanium dioxide (Rhône Poulenc) were weighed as per the stoichiometric ratio and mixed in mortar and pestle using alcohol. The mixture was first calcined at 1200 °C for 24 h, then ground and compacted into a pellet of 40 mm diameter. This compact was then heated at 1350 °C for 24 h, ground and passed through mesh 100.

$Ba_xLa_{0.58(1-x)}Sr_{0.4(1-x)}In_{0.3x}Ti_{0.7x}Co_{0.2(1-x)}Fe_{0.8(1-x)}O_{3-\delta}$ ($0 \leq x \leq 1$) oxide materials have been synthesized by solid state reaction at 1350 °C for 4 h from a mixture of x mol of BIT07 and $(1-x)$ mol of LSCF powders, provided by Marion Technologie. It has been checked by Energy Dispersive X-ray Spectroscopy (EDX) that neither Ba, In nor Co have been volatilized during the synthesis processes.

To simplify the formula, these compounds have been called BLSITCF x where x express the molar ratio (in %) of BIT07 in the initial mixture. Table 1 gathered the initial compositions according to the expected formula. X-ray powder diffraction (XRPD) patterns of these materials were recorded at RT, in Bragg–Brentano reflection geometry using a Brüker “D8 Advance” powder diffractometer with a Cu-anode as X-ray source and equipped with the Vario1, a Johanson type Germanium (111) monochromator that provides pure $K\alpha_1$ radiation ($\alpha = 1.54056 \text{ \AA}$, $20^\circ < 2\theta < 80^\circ$, step = 0.02°) and a 1-D position-sensitive detector (Vantec). Refinements of cell parameters were carried out using the program FULLPROF [17] in the full pattern matching mode, and its interface: the program WinPLOTR [18].

A few selected samples of BLSITCF x were uniaxially pressed under 60 bars in the form of pellets for conductivity and electrochemical characterization, and sintered for 24 h at 1350 °C. Powders were previously ball milled, in 12 ml silicon nitride pot with 6 silicon nitride balls in ethanol, during 4 h at 500 rpm using FRITSCHE P7 planetary micro-mill. XRPD analysis confirms that no contamination occurs during the milling step. Samples with ca 95% apparent density (using both the weight to volume ratio and the theoretical density) were obtained by this process. For DC conductivity measurement, samples were in the form of rectangular bars (5 mm × 0.9 mm × 0.9 mm) which have been cut out from the dense pellet using a diamond saw. Symmetrical half cells have been prepared by screen-printing LSCF, BLSITCF12 or BLSITCF25 on BIT07 using a DEK245 apparatus. Slurries based on a terpeneol – ethyl cellulose vehicle, were screen printed on the two faces of BIT07 dense pellets (surface 0.6 cm² and thickness 0.6 cm) and then heated at

1150 °C for 12 h. One cell was also prepared using a treatment at 1050 °C for 6 h.

2.2. Electrochemical characterization

DC conductivities of LSCF, BLSITCF12, BLSITCF25 and BLSITCF50 were measured in air between 400 °C and 850 °C, after a stabilisation time of 1 h using a DC four points method.

Half cells cathode/electrolyte were characterized by impedance spectroscopy as a function of temperature. The impedance spectra were obtained from a frequency response analyser Solartron 1260 between 450 °C and 700 °C, by steps of 50 °C, with an isotherm of 1 h at each step. Each spectrum has been recorded at open-circuit voltage (OCV), under an ac perturbation of 100 mV and with 84 points scattered in a frequency range from 2 MHz to 0.01 Hz. It has been previously checked that the amplitude of the perturbation signal is small enough to meet the linearity requirement of the transfer function [19].

The evolution of the electrochemical performances versus time was studied using symmetrical half cells maintained at 700 °C for 320 h. Impedance spectra were recorded every 4 h.

2.3. Mechanical properties

Thermal Expansion Coefficients (TECs) have been determined from XRD data as a function of temperature, using a Brüker “D8 Advance” powder diffractometer equipped with an Anton Paar 1200 N high temperature attachment. Data were collected in Bragg–Brentano geometry with a Cu-anode X-ray source ($\lambda_{CuK\alpha 1} = 1.540598 \text{ \AA}$ and $\lambda_{CuK\alpha 2} = 1.544410 \text{ \AA}$, $20^\circ < 2\theta < 80^\circ$, step = 0.02°). Data were recorded every 100 °C from room temperature to 1000 °C. The relation between cell parameters evolution and TEC is:

$$TEC = \frac{1}{3} \times \frac{\left(\delta \left(\frac{\Delta a}{a_0} \right) + \delta \left(\frac{\Delta b}{b_0} \right) + \delta \left(\frac{\Delta c}{c_0} \right) \right)}{\delta T} \quad (1)$$

where a , b and c are the cell parameters at the considered temperature and a_0 , b_0 and c_0 , the cell parameters at room temperature. Refinements of cell parameters were carried out using the program FULLPROF [17] in the full pattern matching mode, and its interface: the program WinPLOTR [18].

The microstructure of the interface cathode/BIT07 has been analysed by Scanning Electron Microscopy (SEM) equipped with an X-ray dispersive spectrometer (JEOL 6400).

3. Results and discussion

3.1. Structural characterization

Fig. 1 shows the X-ray powder diffraction (XRPD) diagrams of the mixture of BIT07 and LSCF in the molar ratio 25/75 before (a) and after 24 h at 1350 °C (b). After the sintering process at 1350 °C, LSCF and BIT07 mixture leads to the formation of a single-phase product which is not a composite. Fig. 1(b) shows, for example, the

Table 1
Molar and weight ratios of BIT07 and LSCF in the initial mixtures, formula and names of the new phases.

| Molar % of BIT07 | Molar % of LSCF | Weight % of BIT07 | Weight % of LSCF | Formula | Material |
|------------------|-----------------|-------------------|------------------|---|-----------|
| 0 | 100 | 0 | 100 | $La_{0.58}Sr_{0.4}Co_{0.2}Fe_{0.8}O_{3-\delta}$ | LSCF |
| 12 | 88 | 13.56 | 86.44 | $Ba_{0.12}La_{0.51}Sr_{0.35}In_{0.04}Ti_{0.08}Co_{0.18}Fe_{0.7}O_{3-\delta}$ | BLSITCF12 |
| 25 | 75 | 27.72 | 72.28 | $Ba_{0.25}La_{0.44}Sr_{0.3}In_{0.08}Ti_{0.18}Co_{0.15}Fe_{0.6}O_{3-\delta}$ | BLSITCF25 |
| 38 | 62 | 41.36 | 58.64 | $Ba_{0.38}La_{0.36}Sr_{0.25}In_{0.11}Ti_{0.27}Co_{0.12}Fe_{0.5}O_{3-\delta}$ | BLSITCF38 |
| 47 | 53 | 50.51 | 49.49 | $Ba_{0.47}La_{0.31}Sr_{0.21}In_{0.14}Ti_{0.33}Co_{0.11}Fe_{0.42}O_{3-\delta}$ | BLSITCF47 |
| 50 | 50 | 53.51 | 46.49 | $Ba_{0.5}La_{0.29}Sr_{0.2}In_{0.15}Ti_{0.35}Co_{0.1}Fe_{0.4}O_{3-\delta}$ | BLSITCF50 |
| 75 | 25 | 77.54 | 22.46 | $Ba_{0.75}La_{0.15}Sr_{0.1}In_{0.23}Ti_{0.53}Co_{0.05}Fe_{0.2}O_{3-\delta}$ | BLSITCF75 |
| 100 | 0 | 0 | 100 | $BaIn_{0.3}Ti_{0.7}O_{2.85}$ | BIT07 |

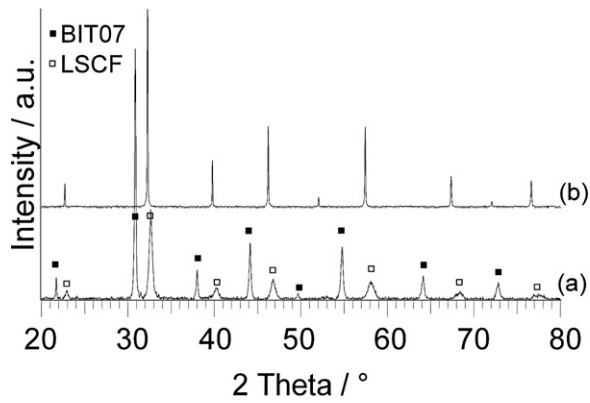


Fig. 1. X-ray powder diffraction patterns of the mixture of BIT07 and LSCF in the molar ratio 25/75 before (a) and after 24 h at 1350 °C (b). Bragg peaks positions of pure BIT07 (■) and LSCF (□) are indicated.

XRPD of BLSITCF25 for which no BIT07 or LSCF peaks are present (Fig. 1(a)). This result could be expected since the precursors BIT07 and LSCF are perovskite type compounds (even if their symmetry is not the same) and shows comparable cell volumes. Similar result has been obtained with the six studied mixtures ($x = 0.12, 0.25, 0.38, 0.47, 0.50$ and 0.75), showing that in all cases single-phase products are obtained, with a regular evolution of the position of the Bragg peaks (Fig. 2). It has been checked by EDX that all the elements of the materials are distributed uniformly in the matrix.

As a consequence, a complete new solid solution is formed between BIT07 and LSCF compositions. The solid solution formula is $\text{Ba}_x\text{La}_{0.58(1-x)}\text{Sr}_{0.4(1-x)}\text{In}_{0.3x}\text{Ti}_{0.7x}\text{Co}_{0.2(1-x)}\text{Fe}_{0.8(1-x)}\text{O}_{3-\delta}$ ($0 \leq x \leq 1$) (Table 1) and is called BLSITCF x where x (in percent) is the molar ratio of BIT07 in the initial composition. Symmetry, refined cell parameters and volume of BLSITCF x are listed in Table 2. As expected, from a structural point of view, a regular evolution of the cell volume is observed between the two limits. A structural transformation from rhombohedral to cubic symmetry occurs for a composition close to BLSITCF20.

3.2. Electrochemical characterization

3.2.1. Total conductivity

The total conductivity of the new phases was measured as a function of temperature using a DC four points method. The evolution of the conductivity level (Fig. 3) does not follow an Arrhenius

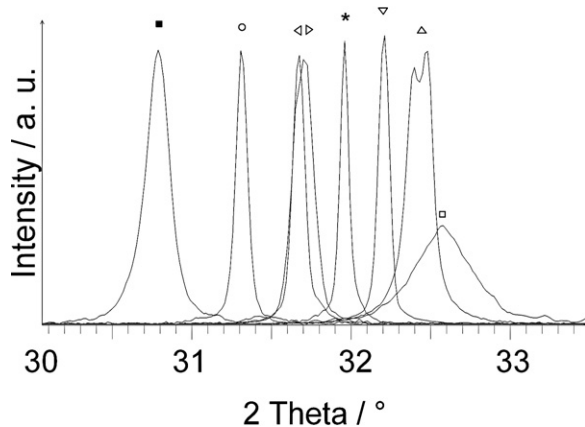


Fig. 2. Evolution of the main X-ray powder diffraction peak position along x in BLSITCF x : cubic (1 1 0) peak for BIT07 (■), BLSITCF75 (○), BLSITCF50 (△), BLSITCF47 (◇), BLSITCF38 (*), BLSITCF25 (▽) and rhombohedral (1 1 0) and (1 0 4) peaks for BLSITCF12 (△) and LSCF (□).

Table 2

Symmetry and refined cell parameters and volumes of the solid solution BLSITCF x .

| Materials | Space group | a (Å) | c (Å) | V (Å ³) |
|-----------|-------------|----------|------------|------------------------|
| LSCF | $R-3c$ | 5.490(1) | 13.4347(1) | 58.445(3) ^a |
| BLSITCF12 | $R-3c$ | 5.522(1) | 13.4737(1) | 59.300(3) ^a |
| BLSITCF25 | $Pm3m$ | 3.927(1) | / | 60.560(3) |
| BLSITCF38 | $Pm3m$ | 3.957(1) | / | 61.958(3) |
| BLSITCF47 | $Pm3m$ | 3.979(1) | / | 62.997(3) |
| BLSITCF50 | $Pm3m$ | 3.991(1) | / | 63.569(3) |
| BLSITCF75 | $Pm3m$ | 4.037(1) | / | 65.792(3) |
| BIT07 | $Pm3m$ | 4.095(1) | / | 68.669(3) |

^a Refers to an equivalent cubic volume.

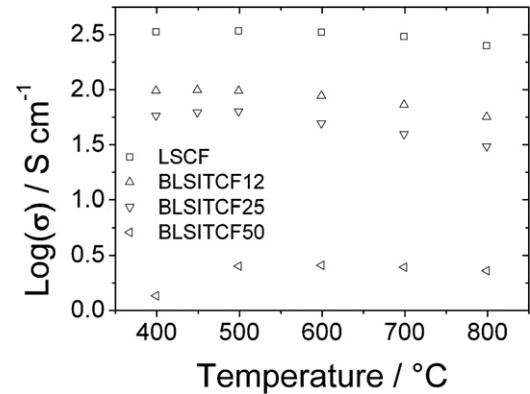


Fig. 3. DC conductivity of LSCF (□), BLSITCF12 (△), BLSITCF25 (▽) and BLSITCF50 (◁).

law but is similar to that already observed for LSCF in the literature [20]. At a given temperature, the conductivity level decreases continuously when x increases in BLSITCF x . For molar ratios of BIT07 in the initial composition superior to 25%, the conductivity values are lower than the target value generally required for a SOFC cathode at 700 °C ($\sim 100 \text{ S cm}^{-1}$) [21].

Based on the results, the compounds BLSITCF75, BLSITCF50, BLSITCF47 and BLSITCF38 cannot be considered as potential cathode materials and are not going to be studied in the following parts of this work.

3.2.2. Electrochemical performances

The two compounds, BLSITCF25 and BLSITCF12, have been studied by complex impedance spectroscopy in air as a function of temperature. Fig. 4 presents the Nyquist diagram obtained at 700 °C for the symmetrical cells BLSITCF12/BIT07/BLSITCF12

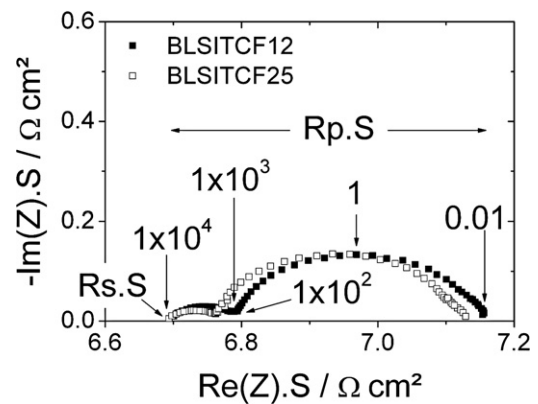


Fig. 4. Nyquist diagram of BLSITCF12/BIT07/BLSITCF12 (■) and BLSITCF25/BIT07/BLSITCF25 (□) symmetrical cell at 700 °C. Characteristic frequencies are reported in Hz. Rs and Rp refer to the series resistance and the polarization resistances respectively.

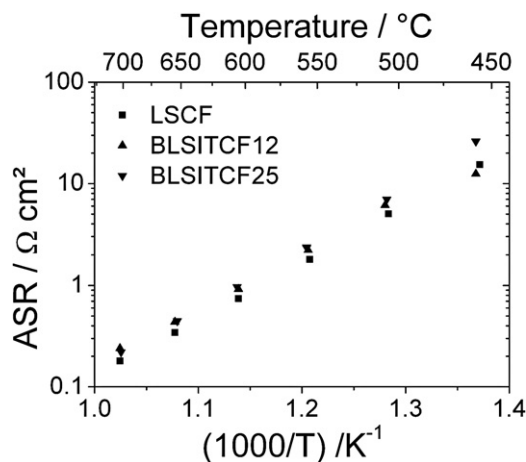


Fig. 5. Arrhenius plots of the total ASR for each symmetrical cell (electrode/BIT07/electrode) when electrode is LSCF (■), BLSITCF12 (▲) and BLSITCF25 (▼).

and BLSITCF25/BIT07/BLSITCF25. It is very similar to that of LSCF previously obtained in the same conditions with the same microstructure [6].

A series resistance, R_s , can be used to model the high frequency part which corresponds mainly to the electrolyte BIT07. Readers can refer to [16] for precisions about BIT07.

At lower frequency two depressed arcs are observed: one at middle frequency (MF) and another one at low frequencies (LF). Each arc was modelled by a $R//CPE$ (CPE for Constant Phase Element) circuit [22] with a capacity around 10^{-5} to 10^{-3} $F\text{ cm}^{-2}$ for the MF contribution and 10^{-1} $F\text{ cm}^{-2}$ for the LF contribution. These MF and LF arcs are usually attributed to the charge transfer and diffusion phenomena, respectively. The polarization resistance, R_p , is the sum of the resistances of the two contributions MF and LF (Fig. 4).

A preliminary study has been made in order to explain the influence of the oxygen partial pressure on the polarization resistance of the three symmetrical cells. Decreasing PO_2 increases drastically the LF contribution which seems to split into two contributions: a third contribution appears at the very low frequencies (VLF), which becomes predominant under very low PO_2 pressure, whatever the material, with a polarization resistance value reaching for instance $50\ \Omega\text{ cm}^2$ at $500\ ^\circ\text{C}$. This result shows that lowering the oxygen concentration leads to a slowing down of the phenomena involved in the low frequency range, confirming that they are correlated to oxygen diffusion. A complete study of the oxygen partial pressure influence on the polarization resistance will be published elsewhere. Concerning the MF contribution, its value is stable, whatever the PO_2 .

The Area Specific Resistance can be deduced from the formula:

$$ASR = \frac{R_p \cdot S}{2} \quad (2)$$

where S (0.5 cm^2) is the cathode surface, R_p is the difference between the two intercepts of the diagram with the real axis at high and low frequencies (see Fig. 4), and the coefficient 2 of the denominator accounts for the fact that the cell is symmetrical.

Fig. 5 presents the total ASR values of the symmetrical cells BLSITCF x /BIT07/BLSITCF x with $x=0, 12$ and 25 . Results are quite similar whatever the composition. The thermal evolution shows an Arrhenius form ($E_a \approx 1\text{ eV}$) and the ASR value does not exceed $0.2\ \Omega\text{ cm}^2$ at $700\ ^\circ\text{C}$.

As previously mentioned, the total ASR value is divided into two contributions called MF and LF. The ratio R/R_p , in which R is associated either to MF or to LF, is reported for LSCF, BLSITCF12 and BLSITCF25 in Fig. 6. Concerning the low frequency contribution, the

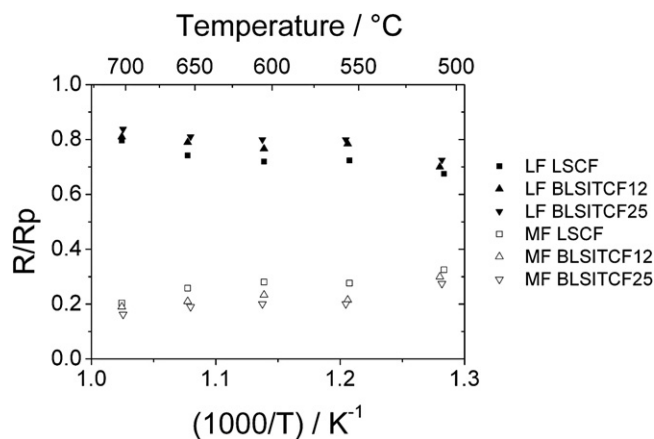


Fig. 6. R/R_p ratio of LSCF/BIT07/LSCF (square), BLSITCF12/BIT07/BLSITCF12 (Δ or \blacktriangle) and BLSITCF25/BIT07/BLSITCF25 (∇ or \blacktriangledown) symmetrical cells versus temperature. R associated to MF and LF contributions are represented by an empty and a filled symbol respectively.

ratio R/R_p for BLSITCF25 is higher than that of LSCF, whereas the MF contribution is smaller. This suggests that in BLSITCF25 the phenomenon associated to charge transfer is faster, whereas diffusion phenomenon is slower. An intermediate situation was observed for BLSITCF12.

Actually, this means that a slight decrease of the ASR can be expected by optimizing the microstructure of the electrode or by reducing its thickness [23]. Then, the diffusion phenomena would be faster [24].

The influence of the electrode microstructure was tested with two symmetrical cells based on BLSITCF12 sintered at $1150\ ^\circ\text{C}$ for 12 h or at $1050\ ^\circ\text{C}$ during 6 h. Lowering the sintering temperature leads to a drastic decrease of the resistance of the LF contribution (Fig. 7), which is divided by a factor 4, whereas the resistance associated to MF remained the same. This suggests that the microstructure of the cathode sintered at $1050\ ^\circ\text{C}$ contributes to a better diffusion of oxygen species. The microstructure shows actually a higher porosity in the case of the electrode sintered at low temperature (Fig. 8). A complete optimization study of each new compound is in progress.

3.3. Mechanical properties

Thermal Expansion Coefficients (TEC) of the new cathode materials selected previously were deduced from XRPD patterns recorded from room temperature to $1000\ ^\circ\text{C}$. These values are gathered in Table 3.

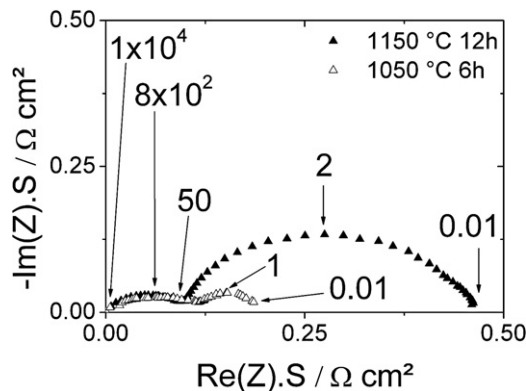


Fig. 7. Nyquist diagrams at $700\ ^\circ\text{C}$ of BLSITCF12/BIT07/BLSITCF12 symmetrical cell where BLSITCF12 was sintered at $1150\ ^\circ\text{C}$ during 12 h (\blacktriangle) or at $1050\ ^\circ\text{C}$ during 6 h (\triangle).

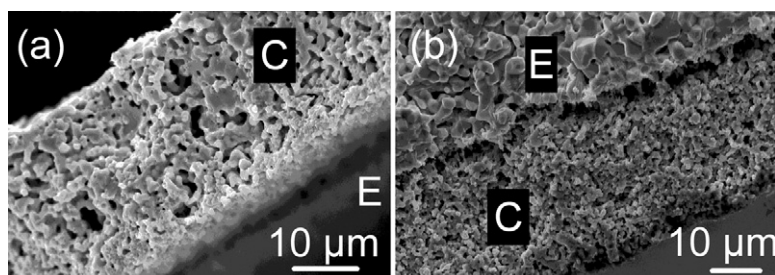


Fig. 8. Scanning electron microscope images of the fracture surface of the BLSITCF12/BIT07/BLSITCF12 symmetrical cells sintered at 1150 °C during 12 h (a) and at 1050 °C during 6 h (b). Cathode and electrolyte have been noted C and E respectively.

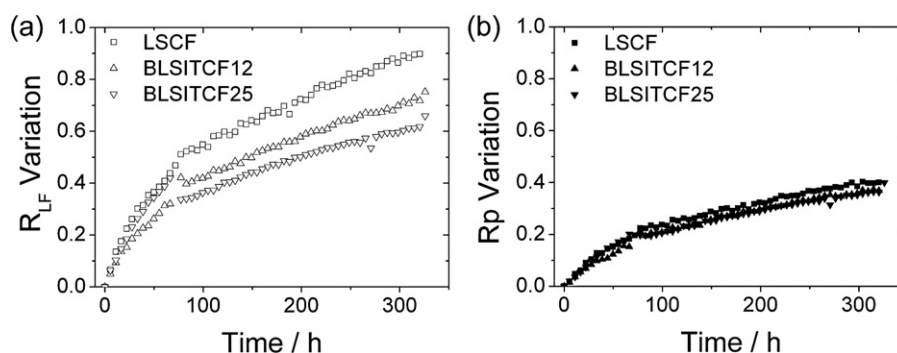


Fig. 9. Resistance evolution with time for the three symmetrical cells (LSCF/BIT07/LSCF (□ or ■), BLSITCF12/BIT07/BLSITCF12 (△ or ▲) and BLSITCF25/BIT07/BLSITCF25 (▽ or ▼): (a) low frequency contribution variation and (b) total variation.

The TEC value of LSCF, obtained by X-ray thermo diffraction ($23.6 \times 10^{-6} \text{ K}^{-1}$) for the temperature range [500–1000 °C] is in agreement with those found in literature [20,25,26], measured by dilatometry and X-ray thermo diffraction as well.

The TEC value decreases linearly with x for BLSITCF x . It means that the TEC mismatch between BIT07 and the new cathode materials is lowered, leading to a very promising conclusion: the lowering of the mechanical mismatch between the electrolyte and the cathode material can lead to an improvement of the ageing behaviour.

3.4. Ageing study

The above studies have shown that the BLSITCF x present similar electrochemical performances and a continuous and significant variation of their TEC. This could have an influence on the ageing of the assembly cathode/electrolyte and especially on its interface. In order to verify this assumption, the behaviour of three symmetrical cells, BLSITCF x /BIT07/BLSITCF x , ($x = 0, 12$ and 25) have been studied by complex impedance spectroscopy as a function of time.

In a recent paper, we have shown that for LSCF at 750 °C, the ASR increases regularly with time [6]. The total resistance R_p and the resistance associated to the low frequency loop (R_{LF}) were measured regularly, and their variations were calculated with the following formula:

$$\text{Variation} = \frac{R - R_0}{R_0} \quad (3)$$

Table 3
Thermal Expansion Coefficients of the studied electrolyte and cathode materials.

| Materials | TEC ($\times 10^{-6} \text{ K}^{-1}$) |
|-----------|---|
| BIT07 | 12.2 (RT–1000 °C) [6] |
| LSCF | 23.6 (500–1000 °C) [6] |
| BLSITCF12 | 21.3 (400–1000 °C) |
| BLSITCF25 | 20.7 (200–1000 °C) |

the subscript 0 corresponding to the initial values. R_{LF} and R_p variations are presented in Fig. 9(a) and (b), respectively for LSCF, BLSITCF12 and BLSITCF25.

As already observed for LSCF [6], the MF contribution of the ASR is nearly constant whereas the LF contribution increases regularly with time. It has been shown above that the MF contribution is less important for BLSITCF12 and BLSITCF25 than for LSCF. So for the new cathode materials, the LF contribution represents a more important part of the polarization resistance than for LSCF. However, after 320 h at 700 °C, the increase of LF contribution is of 90% for LSCF, whereas it is only of 70% and 60% for BLSITCF12 and BLSITCF25, respectively (Fig. 9(a)). These combined effects lead to an equivalent ageing effect for the three materials and even slightly better for the two compounds BLSITCF12 and BLSITCF25 (Fig. 9(b)).

4. Conclusion

New perovskite type oxide materials called BLSICTF x where x corresponds to the molar ratio (in %) of BIT07 in the initial mixture have been successfully synthesized by solid state reaction of BIT07 and LSCF at 1350 °C in air. The solid solution, $\text{Ba}_x\text{La}_{0.58(1-x)}\text{Sr}_{0.4(1-x)}\text{In}_{0.3x}\text{Ti}_{0.7x}\text{Co}_{0.2(1-x)}\text{Fe}_{0.8(1-x)}\text{O}_{3-\delta}$, is complete ($0 \leq x \leq 1$).

Whereas for all BLSITCF x compounds the total conductivity in air is smaller than that of LSCF, BLSITCF12 and BLSITCF25 show conductivity values around 100 S cm^{-1} at 700 °C, and consequently are possible cathode for SOFC. Moreover, in this compositional range ($0 \leq x \leq 0.25$), the TEC value decreases with increasing x in BLSITCF x ($21.3 \times 10^{-6} \text{ K}^{-1}$ and $20.7 \times 10^{-6} \text{ K}^{-1}$ for BLSITCF12 and BLSITCF25, respectively) leading to a lowering of the TEC mismatch between BIT07 and the new cathode materials.

Symmetrical half cells based on BLSITCF12 and BLSITCF25 deposited on BIT07 electrolyte show ASR values lower than $0.2 \Omega \text{ cm}^2$ at 700 °C. However, half cells based on BLSITCF x show an ageing effect at 700 °C during 320 h. A slightly better ageing of

the two compounds BLSITCF12 and BLSITCF25 has been observed, related to the smaller evolution of the LF contribution.

Taking into accounts the results of electrochemical and thermo mechanical analysis, BLSITCF12 seems to be a promising cathode for SOFC with BIT07 as electrolyte, and studies in progress show that an optimization of the microstructure can lead to a further improvement of the polarization resistance.

References

- [1] B.C.H. Steele, *Nature* 400 (1999) 619–621.
- [2] E. Evers-Tiffée, A. Weber, D. Herbristrit, *J. Eur. Ceram. Soc.* 21 (2001) 1805–1811.
- [3] S.C. Singhal, K. Kendall, *High Temperature Solid Oxide Fuel Cells: Fundamentals, Design and Applications*, Elsevier, 2003, p. 197 (chapter 8).
- [4] B.-K. Lai, A.C. Johnson, H. Xiong, S. Ramanathan, *J. Power Sources* 186 (2009) 115–122.
- [5] D. Prakash, T. Delahaye, O. Joubert, M.-T. Caldes, Y. Piffard, *J. Power Sources* 167 (2007) 111–117.
- [6] M. Letilly, A. Le Gal La Salle, M. Marrony, O. Joubert, *Fuel Cells* (2009), doi:10.1002/fuce.200900072.
- [7] H. Ullmann, N. Trofimenko, F. Tietz, D. Stöver, A. Ahmad-Khanlou, *Solid State Ionics* 138 (2000) 79–90.
- [8] F.S. Baumann, J. Fleig, H.U. Habermeier, J. Maier, *Solid State Ionics* 177 (2006) 1071–1081.
- [9] F. Qiang, K. Sun, N. Zhang, X. Zhu, S. Le, D. Zhou, *J. Power Sources* 168 (2007) 338–345.
- [10] Y. Lin, S.A. Barnett, *Solid State Ionics* 179 (2008) 420–427.
- [11] W.G. Wang, M. Mogensen, *Solid State Ionics* 176 (2005) 457–462.
- [12] J.W. Lee, Z. Liu, L. Yang, H. Abernathy, S.H. Choi, H.E. Kim, M. Liu, *J. Power Sources* 190 (2009) 307–310.
- [13] A. Mai, M. Becker, W. Assenmacher, F. Tietz, D. Hathiramani, E. Ivers-Tiffée, D. Stöver, W. Mader, *Solid State Ionics* 177 (2006) 1965–1968.
- [14] J. Chen, F. Liang, L. Liu, S. Jiang, B. Chi, J. Pu, J. Li, *J. Power Sources* 183 (2008) 586–589.
- [15] F. Tietz, *Materials selection for solid oxide fuel cells*, *Mater. Sci. Forum.* 426–432 (2003) 4465–4470.
- [16] T. Delahaye, O. Joubert, M.-T. Caldes, Y. Piffard, P. Stevens, *Solid State Ionics* 177 (2006) 2945–2950.
- [17] Juan Rodríguez-Carvajal, *Phys. B: Condens. Matter* 192 (1993) 55–69, See also <http://www-llb.cea.fr/fullweb/fp2k/fp2k.htm>.
- [18] T. Roisnel, J. Rodríguez-Carvajal, in: R. Delhez, E.J. Mittenmeijer (Eds.), *Materials Science Forum, Proc. of the 7th European Powder Diffraction Conference (EPDIC 7)*, 2000, p. 118, See also <http://www-llb.cea.fr/fullweb/winplotr/winplotr.htm>.
- [19] Q.-A. Huang, R. Hui, B. Wang, J. Zhang, *Electrochim. Acta* 52 (2007) 8144–8164.
- [20] L.-W. Tai, M.M. Nasrallah, H.U. Anderson, D.M. Sparlin, S.R. Sehlin, *Solid State Ionics* 76 (1995) 273–283.
- [21] L.-W. Tai, M.M. Nasrallah, H.U. Anderson, D.M. Sparlin, S.R. Sehlin, *Solid State Ionics* 76 (1995) 259–271.
- [22] S. Ricciardi, J.C. Ruiz-Morales, P. Nunez, *Solid State Ionics* 180 (2009) 1083–1090.
- [23] H. Xiong, B.K. Lai, A.C. Johnson, S. Ramanathan, *J. Power Sources* 193 (2009) 589–592.
- [24] F. Tietz, A. Mai, D. Stöver, *Solid State Ionics* 179 (2008) 1509–1515.
- [25] G. Corbel, S. Mestiri, P. Lacorre, *Solid State Sci.* 7 (2005) 1216–1224.
- [26] K. Świerczek, *Solid State Ionics* 179 (2008) 126–130.